


 Cite this: *RSC Adv.*, 2022, 12, 7085

# Evaporation behavior of $^{233}\text{Pa}$ in FLiBeZr molten salt

 Yuting Huo,<sup>abc</sup> Yan Luo,<sup>bc</sup> Zhongqi Zhao,<sup>bc</sup> Junxia Geng,<sup>bc</sup> Qiang Dou<sup>\*bc</sup> and Jie Ma<sup>id\*<sup>a</sup></sup>

In thorium molten salt reactors (TMSR),  $^{233}\text{Pa}$  is an important intermediate nuclide in the conversion chain of  $^{232}\text{Th}$  to  $^{233}\text{U}$ , its timely separation from the fuel salt is critically important for both the thorium–uranium (Th–U) fuel cycle and the neutron economy of the reactor. In this study, the evaporation behavior of  $^{233}\text{Pa}$  in the FLiBeZr molten salt was investigated during a vacuum distillation process. The separation characteristics between  $^{233}\text{Pa}$  and the major components of the fuel (salt and fission products) were evaluated in a calculation of the separation factors between these components. It was found that  $^{233}\text{Pa}^{5+}$  evaporated more readily than  $^{233}\text{Pa}^{4+}$  and the other components of the fuel, the relatively low temperature and medium pressure were much more beneficial to the separation of  $^{233}\text{Pa}^{5+}$  from FLiBeZr salt in the evaporation process, with the maximum value of the separation factor achieving more than  $10^2$ . Results of distillation experiments also show that increasing the temperature and decreasing the ambient pressure enhances the separation between  $^{233}\text{Pa}^{5+}$  and most of the fission product nuclides due to the  $^{233}\text{Pa}^{5+}$  volatility more strongly depending on the process conditions. These results will be utilized to design a concept for a process for  $^{233}\text{Pa}$  separation from the fuel of a molten salt reactor.

Received 25th November 2021

Accepted 23rd February 2022

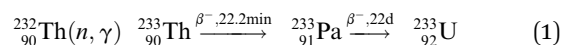
DOI: 10.1039/d1ra08634k

[rsc.li/rsc-advances](https://rsc.li/rsc-advances)

## Introduction

In recent years, energy insecurity and environmental pollution have become two of the greatest threats to human health and economic stability. As conventional fossil fuel supplies are expected to be less available, more expensive and of increasing environmental concern in the coming century, increasing dependence on alternative energy sources is expected.<sup>1</sup> One of the most obvious alternative energy sources is nuclear fission energy, which has incomparable advantages in satisfying our growing need for energy and environmental protection.<sup>2</sup> The molten salt reactor (MSR) is the only liquid-fuel reactor among advanced fourth generation reactors, which uses fluoride salt as both a fuel carrier and reactor coolant.<sup>3,4</sup> The inherent characteristics of the liquid fuel make it can be directly extracted from MSR or added to MSR, so this reactor can achieve online-fuel reprocessing without shutdown.<sup>5</sup> These features of MSR are particularly suitable for the application of thorium in nuclear energy.<sup>6</sup> As a result, MSR has also been recognized as the best type for Th–U fuel cycle. In consequence, thorium molten salt reactor (TMSR) has received extensive research attention in the international nuclear energy field in recent years.<sup>7,8</sup>

In TMSR liquid fuel,  $^{232}\text{Th}$  captures neutrons, which undergo the following nuclear reactions and nuclear decay, transforming into a new fissile nuclide  $^{233}\text{U}$ .<sup>9</sup> The  $^{232}\text{Th}$ – $^{233}\text{U}$  fuel cycle process is shown in eqn (1):



Especially important is  $^{233}\text{Pa}$  (half-life of 27 day), the intermediate nuclide of the  $^{232}\text{Th}$ – $^{233}\text{U}$  fuel cycle.<sup>10</sup> As the thermal neutron capture cross-section of  $^{233}\text{Pa}$  is 5 times higher than that of  $^{232}\text{Th}$ ,  $^{233}\text{Pa}$  gradually accumulated in TMSR fuel would capture considerable neutrons. This will bring dual negative effects: not only consumes important precursor of  $^{233}\text{U}$ , but also reduces the neutron economy of TMSR.<sup>11</sup> In order to maintain efficient operation of the reactor and ensure high breeding of  $^{232}\text{Th}$ ,  $^{233}\text{Pa}$  must be separated from TMSR fuel in time, then could successfully decay into  $^{233}\text{U}$  before being reused.<sup>12</sup> The efficient separation of  $^{233}\text{Pa}$  has received extensive concern and increasing research interest, in line with the strategies of the main countries developing molten salt reactor.

Since 1960s, Oak Ridge National Laboratory (ORNL) had developed the Molten Salt Reactor Experiment (MSRE), and carried out systematic research on fuel treatment of MSR.<sup>13,14</sup> In their fuel reprocessing scenario,  $^{233}\text{Pa}$  would be separated from fuel salt by reductive extraction method, and metal thorium was used as reductant for reductive extraction.<sup>15</sup>  $^{233}\text{PaF}_4$  in salt phase was reduced to metal state by metal thorium, and then extracted in liquid metal bismuth.<sup>16</sup> Finally, the experimental

<sup>a</sup>School of Materials and Chemistry, University of Shanghai for Science and Technology, Shanghai 200093, China. E-mail: majie@usst.edu.cn

<sup>b</sup>Shanghai Institute of Applied Physics, Chinese Academy of Sciences, Shanghai 201800, China. E-mail: douqiang@sinap.ac.cn

<sup>c</sup>Centre of Excellence TMSR Energy System, Chinese Academy of Sciences, Shanghai 201800, China


result clearly shows that the separation coefficient of between  $^{232}\text{Th}$  and  $^{233}\text{Pa}$  can be more than 1500.<sup>17</sup> However, some inherent shortcomings of the reductive extraction method, such as rigorous process requirements and complex equipment system, have presented a formidable challenge for the engineering applications of this method. At the same time, ORNL also investigated the isolation of  $^{233}\text{Pa}$  from fuel salt by oxidation precipitation and had proved in the laboratory scale that  $^{233}\text{Pa}$  could be effectively separated by adding  $\text{BeO}$ ,  $\text{ThO}_2$ ,  $\text{UO}_2$ , and other precipitators to  $\text{LiF-BeF}_2\text{-ThF}_4$  melt.<sup>17,18</sup> As these above-mentioned precipitators were added to salt phase,  $\text{UO}_2\text{-ThO}_2$  solid solution would be formed.  $^{233}\text{Pa}$  can be precipitated by effective contact between salt phase and solid solution. Nevertheless, the fuel salt treated by the oxide precipitation method must be deoxidized and purified before reusing in the reactor, it will greatly increase the workload of fuel treatment of MSR. Consequently, it is still urgent to develop a more effective and convenient method to isolate  $^{233}\text{Pa}$  from the fuel salt. Previous experiments have shown that a certain amount of  $^{233}\text{PaF}_4$  will be produced after  $^{232}\text{ThF}_4$  is irradiated by neutrons. Brookhaven National Laboratory heated the neutron-irradiated  $^{232}\text{ThF}_4$  powder in fluorine gas or chlorine trifluoride gas stream, and found that protactinium compounds evaporated from the powder at 500 °C. In our preliminary experiment, we also found that  $^{233}\text{Pa}$  had certain volatility at high temperature after the fuel salt treated with fluorine gas. So we speculated that  $^{233}\text{Pa}^{4+}$  in fuel salt might be oxidized to pentavalent state by fluorine gas, forming a high volatile protactinium compound. Furthermore, previous study also indicated that pentavalent protactinium was more volatile than  $^{233}\text{Pa}^{4+}$  and sublimed under vacuum above 500 °C.<sup>19,20</sup>

In order to further investigate the feasibility of separation of pentavalent  $^{233}\text{Pa}$  from the fuel salt, the evaporation experiments of fuel salt containing  $^{233}\text{Pa}$  was carried out over a wide temperature and pressure range in this work. This paper would be first to provide the direct comparison of the evaporation behaviours between  $^{233}\text{Pa}$  and molten salt, and address the effect of process conditions on the evaporations of these two substances. Furthermore, in order to investigate the separation between protactinium and the impurity elements in the evaporation process, we systematically detect and compare the radioactivity of  $^{233}\text{Pa}$  and some critical fission product nuclides in the fuel salt before and after evaporation, and the condensed salt. The results in this study are useful and important for both the advance of basic knowledge in the high temperature chemistry of pentavalent protactinium and their potential applications in the efficient separation of  $^{233}\text{Pa}$  from the fuel salt.

## Experimental

### Reagents and materials

$\text{UF}_4$  was purchased from China North Nuclear Fuel Co., Ltd.  $\text{ThF}_4$  with 99.99% purity were provided by the Changchun Institute of Applied Chemistry, Chinese Academy of Sciences, and the oxygen content was 4000 ppm. Fluorine argon mixture (20%) and Ar gas (99.99%) was purchased from Shanghai

Luoyang Gas Co., Ltd. The purity of nickel foil is 99.99% and the thickness of that is 0.03 mm.

### Equipment

$\text{UF}_4$  and  $\text{ThF}_4$  target, loaded separately in sealed acrylic (poly-methyl methacrylate) boxed, were irradiated using a photo-neutron source (PNS) at the Shanghai Institute of Applied Physics, CAS, China. A 15 MeV electronic accelerator send the PNS. The average energy of the neutrons was approximately 1 MeV, the maximum neutron yields reached  $1.2 \times 10^{11} \text{ s}^{-1}$  and total fluence being about  $3 \times 10^{13} \text{ n}$ .  $\text{FLiBeZr}$  molten salt containing irradiated thorium and uranium fluoride was prepared after irradiation and cooling for 24 h.

The experimental equipment used in this work is a self-designed thermogravimetric evaporation furnace, shown in Fig. 1. In order to prevent molten salt from absorbing water and leak radioactive substances, the furnace should be placed in a glove box filled with argon gas (oxygen content  $\leq 10$  ppm, water content  $\leq 100$  ppm). A quartz tube (height = 250 mm, inner diameter = 18 mm, outer diameter 20 mm) is installed in the customized basket. A nickel foil is placed on the quartz tube to collect the vaporized gaseous products, as shown in Fig. 2. Finally, a nickel crucible with height of 25 mm, inner diameter of 14 mm and outer diameter of 16 mm, which is placed at the bottom of the quartz tube.

### Experimental method

First, molten salt for the experiment is prepared.  $\text{LiF-BeF}_2\text{-ZrF}_4$  salt (65–30–5 mol%) was prepared according to the procedures described in our previous work.<sup>21</sup>  $\text{UF}_4$ ,  $\text{ThF}_4$  and  $\text{LiF-BeF}_2\text{-ZrF}_4$  salt with a mass ratio of 2 : 2 : 26 were mixed in the nickel crucible (purity  $\geq 99.96\%$ ), which placed inside the furnace vessel, heated at 550 °C for 3 h, and then 20%  $\text{F}_2/\text{Ar}$  mixture was injected for 2 h. Finally,  $\text{UF}_4$  was oxidized into  $\text{UF}_6$  and then volatilized. The prepared carrier salt ( $\text{FLiBeZr}$ ) containing  $^{233}\text{Pa}$  was cooled and ground into powder for standby application.

Vacuum distillation experiment was carried out in  $\text{FLiBeZr}$  salt. About 1 g of molten salt above was placed in a nickel crucible, which was weighted to record the mass before the experiment and then the radioactivity of the interest nuclides in the molten salt was measured. The crucible is placed at the

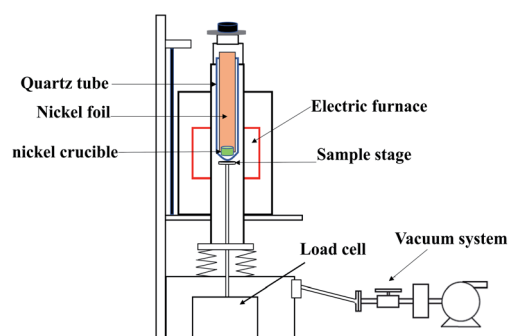


Fig. 1 Schematic diagram of self-designed thermogravimetric evaporation furnace.



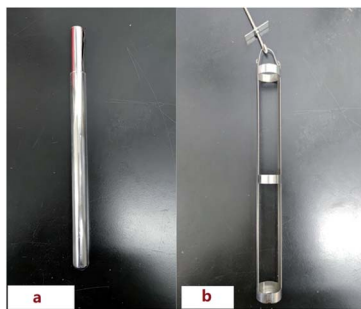


Fig. 2 (a) A ring of nickel foil inside the quartz tube; (b) the customized basket.

bottom of a quartz tube with a ring of nickel foil. Then put the quartz tube in the basket and heat the basket in the thermogravimetric furnace, so that the bottom of the basket is heated at the highest temperature zone of the furnace.

The volatility of  $^{233}\text{Pa}$  before and after fluoridation was compared. The molten salt before and after the fluorination reaction is heated for 1 h at 700, 800, 900 °C respectively and 8 Pa. The evaporation rate of  $^{233}\text{Pa}$  in FLiBeZr molten salt before and after injected fluorine gas was compared. The effect of temperature on  $^{233}\text{Pa}^{5+}$  volatility was studied. The temperature was heated to the experimental temperature (700, 750, 800, 850, 900 °C, respectively) and kept 1 h at 8 Pa. After the evaporation experiment is completed, the mass of the molten salt is weighted, and the activity of the interest nuclides in the remaining molten salt and the molten salt collected by the nickel foil is detected. Next the effect of pressure on  $^{233}\text{Pa}$  volatility was studied. According to the above temperature procedure to keep 850 °C for 1 h and change the pressure into 8, 35, 200, 500,  $10^3$ ,  $10^4$ ,  $10^5$  Pa, respectively. The experimental operation was described above, and then the mass of molten salt and the activity of  $^{233}\text{Pa}$  before and after the experiment were recorded. In this paper, the change of molten salt is calculated with mass. Because of the small amount of  $^{233}\text{Pa}$  and some nuclides in salt, the change of nuclides is calculated with radioactivity. Therefore, in order to make a unified comparison between these two substances, the evaporation percentage per hour is used for comparison.

### Measurement and data analysis

The activity for the radionuclides were measured by a high-purity germanium detector (HPGe) at room temperature. The HPGe detector (model GEM30P4-76-PL) was supplied by ORTEC, USA. The basic nuclear data used for nuclide assignment and activity calculation were provided by ENDF/B-VII.1 (USA, 2011), and listed in Table 1. The uncertainties in activities measured experimentally is the standard deviation, mainly including the statistical errors in  $\gamma$ -ray counts, a 4–6% error in detector efficiency and a 6% error in sample geometry. Generally, the typical uncertainty of  $^{233}\text{Pa}$  is 7–13%, and other given nuclides are approximately 15% or less.

From the beginning of the vacuum distillation experiment to the measurement of radioactivity after the experiment, the

influence of the radioactive decay on the accuracy of radioactivity calculation is obvious enough not to be ignored. Therefore, the calculation of radioactivity in this paper used the exponential decay law formula to eliminate the influence of the radioactive decay during this period, so as to ensure the accuracy of the calculation result of the separation factor.<sup>22</sup>

On studying the separation of  $^{233}\text{Pa}$  from fission products, the minimum detectable activity (MDA) in units of Bq for some selected nuclides is calculated as follows eqn (2):<sup>23</sup>

$$\text{MDA} = \frac{2.71 + 4.65\sqrt{N_b}}{\varepsilon(E)\gamma(E)t} \quad (2)$$

where is the background count in the total-energy peak region of  $\gamma$ -rays;  $\varepsilon(E)$  is the deviation efficiency of ray energy  $E$ ;  $\gamma(E)$  is the branching ratio of ray energy  $E$ ;  $T$  is the measured live time.

## Results and discussions

To our knowledge, protactinium is usually present as tetravalent state in TMSR fuel,<sup>15</sup> but in our previous experiment, we found that  $^{233}\text{Pa}$  in the molten salt after fluoridation became more volatile, indicating that the effect of the valence states of protactinium on its volatility is significant. In order to further investigate the difference of  $^{233}\text{Pa}$  evaporation behaviours in the fuel salts before and after fluoridation, we performed evaporation experiments in these two kinds of fuel salt at 8 Pa and at a given temperature (700, 800, or 900 °C). The obtained results are shown in Fig. 3, from which it is seen clearly that the evaporation rates of  $^{233}\text{Pa}$  in the salts before fluoridation were 0, 12, 40%/h respectively with the evaporation temperature increasing, whereas the evaporation rates of fuel salt were 0.65, 5.14 and 36%/h, respectively. This result indicates that tetravalent protactinium and FLiBeZr molten salt have similar volatility at different temperatures. On the other hand, it also can be found in Fig. 3 that when the molten salt had been treated by fluorine gas, the evaporation rates of  $^{233}\text{Pa}$  were greatly improved in the temperature range studies, while the changes of the evaporation rates of FLiBeZr molten salt is negligible. So we speculate that protactinium in the salt after fluoridation is likely to present as pentavalent state with higher volatility. Consequently, this paper will mainly address the evaporation behaviour of  $^{233}\text{Pa}^{5+}$  in fuel salt during vacuum distillation at high temperature, focusing on the effects of process conditions on the evaporation behaviour of  $^{233}\text{Pa}$ , and the separation behaviour between  $^{233}\text{Pa}$  and a variety of fission product in the evaporation.

### The effect of temperature on the evaporation behavior of $^{233}\text{Pa}^{5+}$

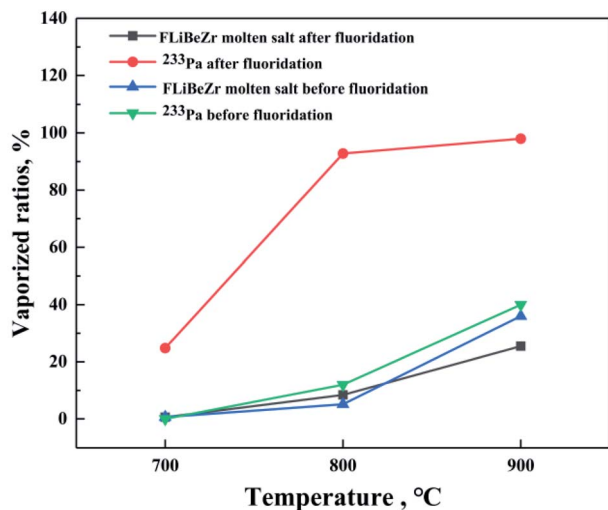
Temperature is one of the most important factors affecting the evaporation of substances. The evaporation rate of a given substance can be calculated by the Langmuir–Knudsen relation derived from the theory of gas dynamics, as shown in eqn (3).<sup>24</sup>

$$G = \frac{1}{\sqrt{2\pi R}} P \sqrt{\frac{M}{T}} \quad (3)$$



Table 1 Nuclear data of the nuclides relevant to this work

Nuclide	Energy/keV	Intensity/%	Energy/keV	Intensity/%	Energy/keV	Intensity/%
$^{233}\text{Pa}$	311.9	38.5	300.1	6.63	340.5	4.45
$^{95}\text{Nb}$	765.8	99.81	561.9	0.015	—	—
$^{103}\text{Ru}$	497.1	91.0	610.3	5.76	—	—
$^{141}\text{Ce}$	145.4	48.29	—	—	—	—
$^{140}\text{Ba}$	537.3	24.39	162.6	6.219	304.8	4.293
$^{95}\text{Zr}$	756.7	54.38	724.2	44.27	—	—

Fig. 3 The vaporized ratios of FLiBeZr salt and  $^{233}\text{Pa}$  as a function of temperature.

where  $G$  is the evaporation rate in  $\text{kg m}^{-2} \text{s}^{-1}$ ,  $P$  is the vapor pressure in Pa,  $M$  is the molar weight in  $\text{J mol}^{-1} \text{K}^{-1}$ ,  $R$  is the ideal gas constant in 8.314,  $T$  is the absolute temperature in K. The  $P$  mentioned here strongly depends on the evaporation temperature. A series of evaporation experiments were performed to explore the evaporation behaviour of  $^{233}\text{Pa}^{5+}$  in the fluorinated fuel salt at 8 Pa and at temperatures ranging from 700 to 900 °C. Fig. 4 shows the vaporized ratios of  $^{233}\text{Pa}^{5+}$  and the molten salt as functions of temperature. It can be found that the evaporation rate of  $^{233}\text{Pa}$  shows a sharp increase (from 17.92%/h to 80.26%/h) below 800 °C, but that of the molten salt increases slowly. As the temperature increases continuously, a dramatic reversal appears in the trend of this two evaporation rate curves. The above results indicated that the effects of temperature on the evaporation behaviour of FLiBeZr salt and  $^{233}\text{Pa}$  are significantly different.

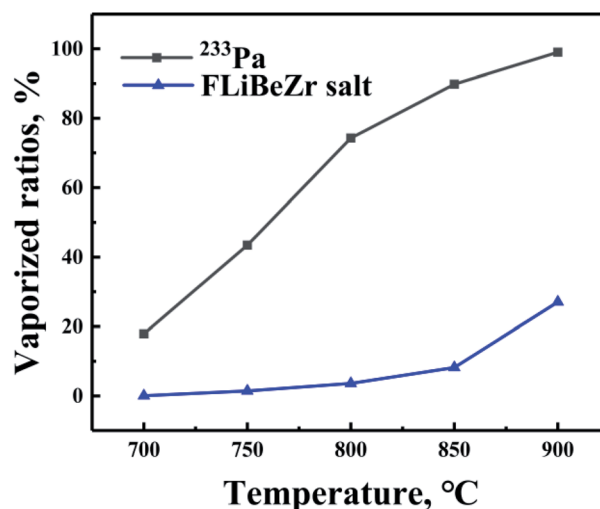
In order to achieve the efficient separation of  $^{233}\text{Pa}$  from the fuel salt, it is necessary to explore the difference in the volatility of  $^{233}\text{Pa}^{5+}$  and FLiBeZr salt over a wide temperature range. Therefore, the concept of separation coefficient was used to evaluate the separation behaviour between  $^{233}\text{Pa}$  and FLiBeZr salt in the high-temperature evaporation. The separation coefficient,  $\Phi$ , was calculated based on the radioactivity of  $^{233}\text{Pa}$  and the mass of the molten salt before evaporation and on nickel foil after evaporation, as shown in eqn (4):

$$\Phi = \frac{m^0/A^0}{m'/A'} \quad (4)$$

where  $A^0$  is the activity of  $^{233}\text{Pa}$  before evaporation, in units of Bq;  $m^0$  is the total mass of FLiBeZr salt before evaporation, in g;  $A'$  is the activity of  $^{233}\text{Pa}$  on nickel foil after evaporation, in Bq;  $m'$  is the mass of salt in nickel foil after evaporation, in g. On the basis of the data in Fig. 5, it is found that although the volatility of  $^{233}\text{Pa}^{5+}$  is obviously higher than that of FLiBeZr salt at any given temperature, and the separation coefficients strongly depend on the temperature, with the maximum value of  $\Phi$  (near 300) appearing at 700 °C. Since the evaporation of FLiBeZr salt is intensified with the increase of temperature,  $\Phi$  of these two substances decreases sharply. Therefore, the relatively low temperature is more conducive to the separation of  $^{233}\text{Pa}$  and FLiBeZr salt in the evaporation process.

#### The effect of pressure on the evaporation behaviour of $^{233}\text{Pa}^{5+}$

Ambient pressure is another important factor affecting the evaporation of substances. Generally, the evaporation rate of substances will increase greatly as the pressure drops to a sufficiently low level. In order to investigate the effect of pressure on the evaporation behaviour of  $^{233}\text{Pa}^{5+}$  in the molten salt, a series of evaporation experiments have been performed using simulated fuel salt under the ambient pressures ranging

Fig. 4 Vaporized ratios of  $^{233}\text{Pa}$  and FLiBeZr salt as a function of temperature.

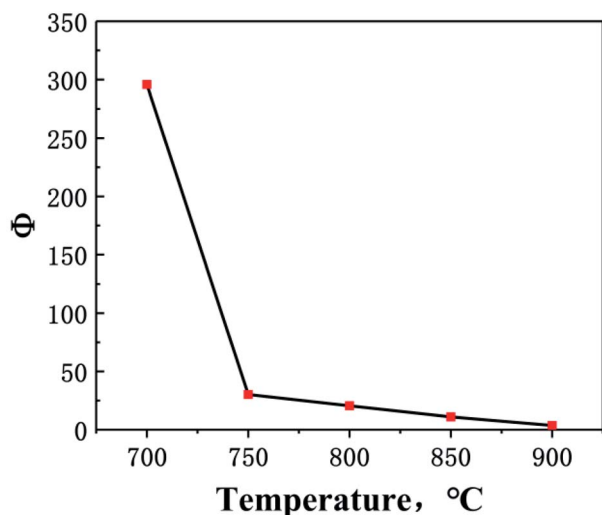


Fig. 5 The separation coefficient,  $\Phi$ , as a function with temperature.

from 8 Pa to  $10^5$  Pa. Fig. 6 represents the vaporized ratios of  $^{233}\text{Pa}^{5+}$  and the molten salt as functions of pressure.

From Fig. 6 it is evident that  $^{233}\text{Pa}$  is non-volatile at normal pressure ( $10^5$  Pa), with the evaporation rate of FLiBeZr salt only 0.22%/h. As the ambient pressure decreases continuously, the evaporation rate of  $^{233}\text{Pa}$  shows a sharp increase (from 29.43%/h to 99.83%/h) below 1000 Pa. By contrast, the evaporation rate of the salt not show a significant increase until the pressure drops below 100 Pa. A key factor responsible for this difference in their evaporation behaviours may lie in their own volatility. Previous theoretical and experimental studies in high temperature melts have shown that when ambient pressure decreases continuously, the evaporation rate of the melts would not present a sharply increase until the pressure approaches its vapor pressure.<sup>25,26</sup> The preceding experimental studies have shown that the vapor pressure of FLiBeZr salt is just around 10–

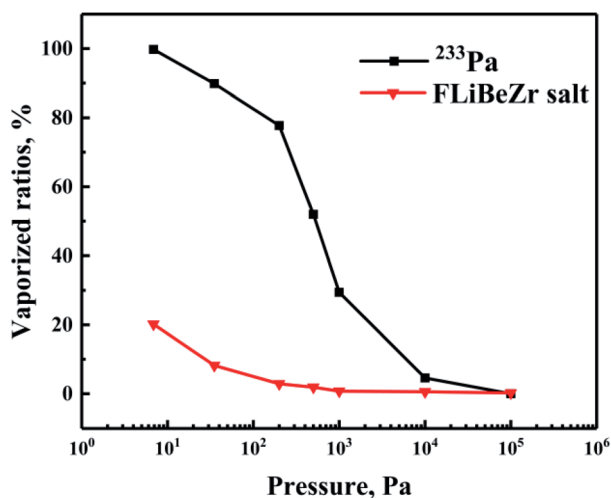


Fig. 6 Vaporized ratios of  $^{233}\text{Pa}$  and FLiBeZr salt, at 850 °C, as a function of pressure.

100 Pa,<sup>16</sup> which is much close to the transition pressure of this salt shown in Fig. 6. On the basis of the data in Fig. 6, we can also draw a reasonable speculation that the vapor pressure of  $^{233}\text{Pa}^{5+}$  in the melt is near 1000 Pa, which is obviously higher than of the melt.

Hence, in order to further characterize the effect of ambient pressure on the separation between FLiBeZr salt and  $^{233}\text{Pa}^{5+}$ , we also calculate the separation coefficient,  $\Phi$  of these two substances in the pressure range studies, as shown in Fig. 7.  $\Phi$  increases sharply first and then decreases with decreasing of ambient pressures, and the maximum value (about 43) is observed at 1000 Pa. It is thus evident that the medium pressure, such as about 1000 Pa, can effectively inhibit the evaporation of FLiBeZr salt and is much more beneficial to the separation of  $^{233}\text{Pa}$  from the molten salt.

### The separation of protactinium and fission products

On the basis of the above results, it is found that most of the  $^{233}\text{Pa}^{5+}$  can vaporize from fuel salt efficiently under high temperature and low pressure. However, part of the fission products in the TMSR fuel may also be volatile and evaporate into gas phase along with the  $^{233}\text{Pa}^{5+}$ . Therefore, understanding the separation behaviour between  $^{233}\text{Pa}$  and various fission products is an important step towards the recovery and the purification of  $^{233}\text{Pa}$ .

Therefore, to get insight into the evaporation of these nuclides during vacuum distillation, we performed in distillation experiments in this work at temperatures ranging from 700–900 °C with evaluating the  $\gamma$ -activity changes of these critical nuclides in the fuel salt before and after distillation. Fig. 8 represents that the  $\gamma$ -activity of  $^{233}\text{Pa}$  and fission product nuclides in the fuel salts before and after distillation. It can be seen that the volatility of  $^{233}\text{Pa}$  increases sharply with increasing evaporation temperature. However,  $^{95}\text{Nb}$  and  $^{95}\text{Zr}$  do not vaporized until the evaporation temperature rises above 800 °C. Under the same conditions, the  $\gamma$ -activity of  $^{141}\text{Ce}$ ,  $^{140}\text{Ba}$  and

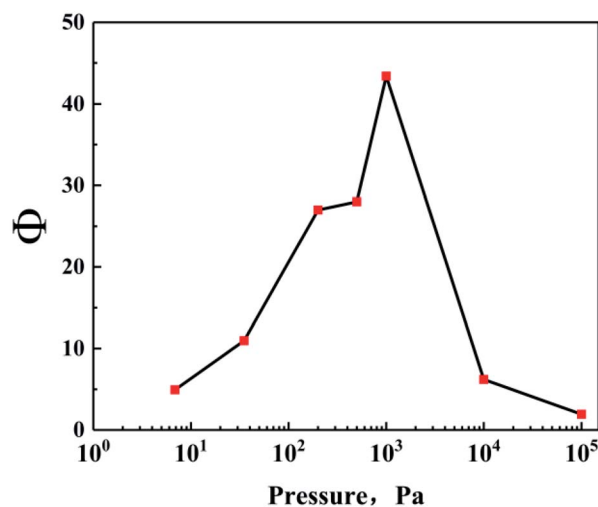


Fig. 7 The separation coefficient,  $\Phi$ , as a function of pressure.



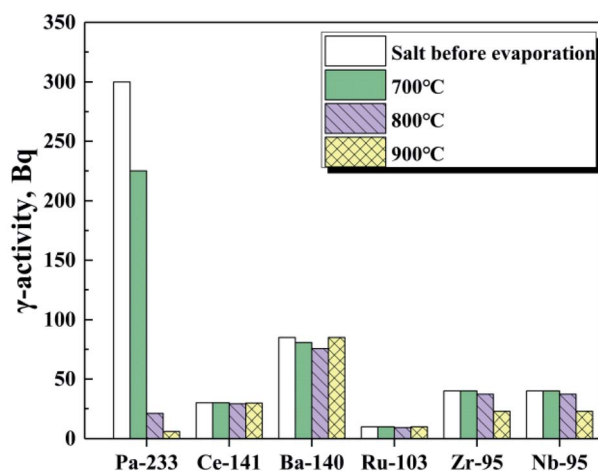


Fig. 8 The  $\gamma$ -activity of each element in the remaining FLiBeZr salt, at 850 °C, as a function of temperature.

Table 2 The separation coefficient of  $^{233}\text{Pa}$  and these nuclides at 8 Pa, and 700, 800, 900 °C respectively

	$\beta_{(\text{Ce}/\text{Pa})}$	$\beta_{(\text{Ba}/\text{Pa})}$	$\beta_{(\text{Ru}/\text{Pa})}$	$\beta_{(\text{Zr}/\text{Pa})}$	$\beta_{(\text{Nb}/\text{Pa})}$
700 °C	87	13	25	31	19
800 °C	184	41	63	127	86
900 °C	323	42	94	102	143

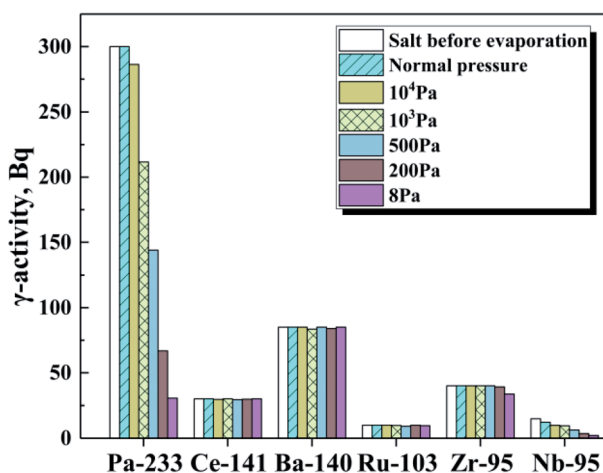


Fig. 9 The  $\gamma$ -activity of each element in the remaining FLiBeZr salt, at 850 °C, as a function of pressure.

$^{103}\text{Ru}$  is not influenced by the evaporation process, indicating that these fission products are non-volatile in the temperature range studied. Separation factor is used to be defined as the process separability between two components of reference and impurity.<sup>27</sup> In order to further characterize the separation behaviour between  $^{233}\text{Pa}$  and these critical fission products, the separation factor,  $\beta_{(i/\text{Pa})}$ , between these nuclides was calculated based on the activity data of relevant nuclides in fuel salts before evaporation and on nickel foil after evaporation respectively, and list in Table 2. The  $\beta_{(i/\text{Pa})}$  of  $^{233}\text{Pa}$  in TMSR fuel salt

Table 3 The separation coefficient of  $^{233}\text{Pa}$  and these nuclides at 850 °C and different pressure

	$\beta_{(\text{Ce}/\text{Pa})}$	$\beta_{(\text{Ba}/\text{Pa})}$	$\beta_{(\text{Ru}/\text{Pa})}$	$\beta_{(\text{Zr}/\text{Pa})}$	$\beta_{(\text{Nb}/\text{Pa})}$
8 Pa	75	296	26	6	2
200 Pa	57	91	9	38	1
500 Pa	39	43	10	343	2
$10^3$ Pa	3	9	2	10	0.18
$10^4$ Pa	10	17	3	78	0.33
Normal pressure	1	1	1	1	0.002

with respect to a specified nuclide were calculated by the following formula eqn (5):

$$\beta_{(i/\text{Pa})} = \frac{x_{i0}/x_{\text{Pa}0}}{x_{i1}/x_{\text{Pa}1}} \quad (5)$$

where  $x_{i0}$  and  $x_{i1}$  are the  $\gamma$ -activity of a given nuclides  $i$  in FLiBeZr salt before evaporation and on nickel foil after evaporation;  $x_{\text{Pa}0}$  and  $x_{\text{Pa}1}$  is the  $\gamma$ -activity of  $^{233}\text{Pa}$  in the FLiBeZr salt before evaporation and on nickel foil after evaporation. As seen in Table 2,  $\beta_{(\text{Ce}/\text{Pa})}$ ,  $\beta_{(\text{Ba}/\text{Pa})}$ ,  $\beta_{(\text{Ru}/\text{Pa})}$  gradually increases with increasing evaporation temperature due to the temperature dependence of the  $^{233}\text{Pa}^{5+}$  volatility. Although the volatility of  $^{95}\text{Nb}$  and  $^{95}\text{Zr}$  also shows temperature dependent as well as that of  $^{233}\text{Pa}^{5+}$  (see Fig. 8), on the basis of the data in Table 2, it is found that the higher temperature is obviously more beneficial to the separation of  $^{233}\text{Pa}$  and  $^{95}\text{Nb}$ ,  $^{95}\text{Zr}$ , and  $\beta_{(\text{Nb}/\text{Pa})}$ ,  $\beta_{(\text{Zr}/\text{Pa})}$  are more than 100.

Next, to get insight into the effect of pressure on the separation distillation experiments were performed under the ambient pressures ranging from 8 Pa to  $10^5$  Pa by using the simulated fuel salt. The  $\gamma$ -activity of these nuclides in the molten salt before and after distillation are shown in Fig. 9, and it is found that at normal pressure  $^{95}\text{Nb}$  is only nuclides which shows obvious volatility. As the ambient pressure decreases continuously,  $^{233}\text{Pa}$  begins to volatilize at  $10^4$  Pa, and  $^{95}\text{Zr}$  does not show obvious volatility until the pressure drops to 200 Pa. Meanwhile, we also found that  $^{141}\text{Ce}$ ,  $^{140}\text{Ba}$ ,  $^{103}\text{Ru}$  are almost non-volatile and not influenced by the pressure in these distillation experiments. The  $\beta_{(i/\text{Pa})}$  between  $^{233}\text{Pa}$  and these nuclides at different pressure were also calculated by using the  $\gamma$ -activity of relevant nuclides in FLiBeZr salt before distillation and on nickel foil after distillation, listed in Table 3. Since  $^{233}\text{Pa}$ ,  $^{141}\text{Ce}$ ,  $^{140}\text{Ba}$ ,  $^{95}\text{Zr}$ , and  $^{103}\text{Ru}$  are not volatile at normal pressure, the  $\beta$  values between them is basically 1. But the evaporation rate of  $^{95}\text{Nb}$  reaches 18%/h, and  $\beta_{(\text{Nb}/\text{Pa})}$  is 0.002, indicating that the separation of  $^{233}\text{Pa}$  and  $^{95}\text{Nb}$  can be achieved at normal pressure. With the decrease of pressure, the  $\beta$  values between  $^{233}\text{Pa}$  and the non-volatile fission products, such as  $^{141}\text{Ce}$ ,  $^{140}\text{Ba}$  and  $^{103}\text{Ru}$ , increase sharply, reaching the highest values of 75, 296 and 26 at 8 Pa, respectively. Since  $^{95}\text{Zr}$  shows obvious volatility at 200 Pa, the maximum separation factor  $\beta_{(\text{Zr}/\text{Pa})}$  (343) is observed at 500 Pa.

## Conclusions

In this study, the evaporation behavior of  $^{233}\text{Pa}$  in the simulated fuel salt was investigated during a vacuum distillation process.



The separation characteristics between  $^{233}\text{Pa}$  and the major components of the fuel were evaluated in these vacuum distillation experiments. Meanwhile, the valence state, temperature and ambient pressure effects on the separation behavior of  $^{233}\text{Pa}$  had been estimated systematically. Our experiment results clearly show that  $^{233}\text{Pa}^{5+}$  evaporates more readily than  $^{233}\text{Pa}^{4+}$  and the fuel salt, the relatively low temperature and medium pressure were much more beneficial to the separation of  $^{233}\text{Pa}^{5+}$  from FLiBeZr salt. The separation factor between  $^{233}\text{Pa}^{5+}$  and the molten salt can easily achieve more than  $10^2$ .

Understanding the separation behavior between  $^{233}\text{Pa}$  and the critical fission products is an important step towards the recovery and the purification of  $^{233}\text{Pa}$ . The experimental results suggest that the difference in the volatility between  $^{233}\text{Pa}^{5+}$  and these fission product nuclides increases with temperature, and lower pressure is more conducive to the separation of  $^{233}\text{Pa}$  and the non-volatile fission products ( $^{141}\text{Ce}$ ,  $^{140}\text{Ba}$  and  $^{103}\text{Ru}$ ). In contrast,  $^{95}\text{Nb}$  can be well separated from  $^{233}\text{Pa}$  at normal pressure. The results in this study would be useful and important for the understanding of the physicochemical property of  $^{233}\text{Pa}$  in the molten salt and for the design of a process for  $^{233}\text{Pa}$  separation from the TMSR fuel.

## Conflicts of interest

There are no conflicts to declare.

## Acknowledgements

This work was supported by the "National Natural Science Foundation of China" (grant no 21601201.).

## References

- 1 J.-L. Wang, J.-X. Feng, Y. Bentley, L.-Y. Feng and H. Qu, *Pet. Sci.*, 2017, **14**, 806–821.
- 2 A. Horvath and E. Rachlew, *AMBIO*, 2016, **45**(suppl 1), S38–S49.
- 3 J. Serp, M. Allibert, O. Beneš, S. Delpech, O. Feynberg, V. Ghetta, D. Heuer, D. Holcomb, V. Ignatiev, J. L. Kloosterman, L. Luzzi, E. Merle-Lucotte, J. Uhlíř, R. Yoshioka and D. Zhimin, *Prog. Nucl. Energy*, 2014, **77**, 308–319.
- 4 O. Benes and R. J. M. Konings, *J. Fluorine Chem.*, 2009, **130**, 22–29.
- 5 A. Rykhlevskii, J. W. Bae and K. D. Huff, *Ann. Nucl. Energy*, 2019, **128**, 366–379.
- 6 M. B. Schaffer, *Energy Policy*, 2013, **60**, 4–12.
- 7 O. Ashraf, A. Rykhlevskii, G. V. Tikhomirov and K. D. Huff, *Ann. Nucl. Energy*, 2020, 148.
- 8 A. Nuttin, D. Heuer, A. Billebaud, R. Brissot, C. Le Brun, E. Liatard, J. Loiseaux, L. Mathieu, O. Meplan and E. Merle-lucotte, *Prog. Nucl. Energy*, 2005, **46**(1), 77–99.
- 9 K. Furukawa, K. Arakawa, L. B. Erbay, Y. Ito, Y. Kato, H. Kiyavitskaya, A. Lecocq, K. Mitachi, R. Moir, H. Numata, J. P. Pleasant, Y. Sato, Y. Shimazu, V. A. Simonenco, D. D. Sood, C. Urban and R. Yoshioka, *Energy Convers. Manage.*, 2008, **49**, 1832–1848.
- 10 D. Leblanc, *Nucl. Eng. Des.*, 2009, **240**, 1644–1656.
- 11 R. G. Ross, C. Bamberger and C. F. Baes Jr, *J. Inorg. Nucl. Chem.*, 1973, **35**(2), 433–449.
- 12 S. Zhou, W. S. Yang, T. Park and H. Wu, *Ann. Nucl. Energy*, 2018, **114**, 369–383.
- 13 R. C. Robertson, *Conceptual Design Study of a Single-Fluid Molten Salt Breeder Reactor*, 1971.
- 14 J. Uhlíř, *J. Nucl. Mater.*, 2007, **360**(1), 6–11.
- 15 M. E. Whatley, L. E. McNeese, W. L. Carter, L. M. Ferris and E. L. Nicholson, *Nucl. Appl. Technol.*, 2017, **8**, 170–178.
- 16 R. W. Grimes, *Reactor Chemistry Division Annual Progress Report For Period Ending January 31, 1965*, 1965.
- 17 W. R. Grimes, *Nucl. Appl. Technol.*, 2017, **8**, 137–155.
- 18 J. H. Shaffer, W. R. Grimes, G. M. Watson, D. R. Cuneo, J. E. Strain and M. J. Kelly, *Nucl. Sci. Eng.*, 2017, **18**, 177–181.
- 19 N. E. Agency, *Spent Nuclear Fuel Reprocessing Flowsheet*, 2012.
- 20 L. Stein, *Inorg. Chem.*, 1967, **3**, 995–998.
- 21 D. Han, C. She, Y. Niu, X. Yang, J. Geng, R. Cui, L. Sun, C. Hu, Y. Liu and T. Su, *J. Radioanal. Nucl. Chem.*, 2019, **319**, 899–906.
- 22 W. B. Guenther, *J. Chem. Educ.*, 1958, **35**, 414.
- 23 L. Done and M.-R. Ioan, *Applied radiation and isotopes: including data, instrumentation and methods for use in agriculture, industry and medicine*, 2016.
- 24 H. C. Eun, H. C. Yang, Y. Z. Cho, H. S. Park, H. S. Lee and I. T. Kim, *J. Radioanal. Nucl. Chem.*, 2009, **280**, 643–649.
- 25 H. C. Yang, H. C. Eun and I. T. Kim, *Vacuum*, 2009, **84**(5), 751–755.
- 26 Y. Dai and B. Yang, *Vacuum Metallurgy of Non Ferrous Metals*, Metallurgical Industry Press (in Chinese), Beijing, 2000.
- 27 E. B. Sandell, *Anal. Chem.*, 1968, **40**(4), 834–835.

